

Crucial role of thermal fluctuations and vertex corrections for the magnetic pseudogap

Mengxing Ye^{1,2} and Andrey V Chubukov³

¹*Kavli Institute for Theoretical Physics, University of California, Santa Barbara, CA 93106, USA*

²*Department of Physics and Astronomy, University of Utah, Salt Lake City, UT 84112, USA*

³*School of Physics and Astronomy and William I. Fine Theoretical Physics Institute, University of Minnesota, Minneapolis, MN 55455, USA*

(Dated: September 13, 2023)

It is generally believed that in a 2D metal, whose ground state is antiferromagnetically ordered with $\mathbf{Q} = (\pi, \pi)$, thermal (static) magnetic fluctuations give rise to precursor behavior above T_N , in which the spectral function of a hot fermion (the one for which \mathbf{k} and $\mathbf{k} + \mathbf{Q}$ are Fermi surface points) contains two peaks, separated by roughly the same energy as in the antiferromagnetically ordered state. The two peaks persist in some range of $T > T_N$ and eventually merge into a single peak at zero frequency. This behavior is obtained theoretically by departing from free fermions in a paramagnet and evaluating the dressed fermionic Green's function by summing up infinite series of diagrams with contributions from thermal magnetic fluctuations. We show, following [Y.M. Vilk and A.-M. S. Tremblay, *J. Phys. I France* **7** 1309 (1997)] that keeping vertex renormalization diagrams in these series is crucial as other terms only broaden the spectral function of a hot fermion, but do not shift its maximum away from zero frequency. As the consequence, the magnetic pseudogap should be treated as an input for theories that neglect vertex corrections, like, e.g., Eliashberg theory for magnetically-mediated superconductivity. We also analyze the potential pseudogap behavior at $T = 0$. We argue that it may exist, but only at a finite correlation length, and not as a precursor to antiferromagnetism.

Introduction. The origin of the pseudogap behavior, observed in the cuprates and other correlated materials remains the subject of ongoing debate. Theoretical proposals for the pseudogap can be broadly split into three categories. One identifies pseudogap behavior with some particle-hole order, either a conventional one, like a charge-density wave (CDW) [1–5], or less conventional, like a circulating current [6, 7]. Another identifies the pseudogap with a spin-liquid-type “mother” state, from which one gets antiferromagnetism, superconductivity, and charge order [8–12]. And the third treats the pseudogap phase as a precursor to an ordered state - either a spin-density-wave (SDW) order [13–30], or superconductivity [20, 31–37], or pair-density-wave [38].

In this communication we focus on the last category and discuss some aspects of a precursor to an SDW order with $\mathbf{Q} = (\pi, \pi)$ in two dimensions. We analyze the emergence of peaks at a finite frequency in the spectral function of a fermion on the Fermi surface, particularly at a hot spot \mathbf{k}_{hs} , for which \mathbf{k}_{hs} and $\mathbf{k}_{hs} + \mathbf{Q}$ are both on the Fermi surface. The emergence of such peaks without a full gap between them is a signature feature of pseudogap behavior.

We address two issues. The first is about pseudogap behavior caused by thermal magnetic fluctuations [14, 16–20, 22, 23, 25–28, 30]. Several groups, including us, demonstrated [16, 17, 19, 20, 22, 25, 30] that that pseudogap does develop when one includes infinite series of contributions to the fermionic Green's function

from thermal (static) spin fluctuations. In this communication, we look more closely at the interplay between non-crossed and crossed diagrams in these series. The non-crossed diagrams renormalize the Green's function of an intermediate fermion, $G_0(\mathbf{k}+\mathbf{q}, \omega_m) \rightarrow G(\mathbf{k}+\mathbf{q}, \omega_m)$, and can be absorbed into the self-consistent one-loop theory (SCOLT). The crossed diagrams describe vertex corrections. Previous studies [13, 14, 18, 26] found that at large dimensionless spin-fermion coupling λ_{th} , the non-crossed diagrams, taken alone, broaden the spectral function of a hot fermion, but the maximum remains at $\omega = 0$, i.e., pseudogap does not emerge. Here, we show that (i) pseudogap behavior does not develop within SCOLT for any value of λ_{th} , (ii) SCOLT is the “boundary” case in the sense that already infinitesimally small vertex corrections give rise to a pseudogap, and (iii) SCOLT is a member of a one-parameter set of such boundary models, which do not display pseudogap behavior, but develop it upon an infinitesimally small perturbation.

Second, we analyze whether the system can potentially display pseudogap behavior at $T = 0$. We argue that this holds in the weak coupling regime away from the SDW quantum-critical point (QCP), when SDW fluctuations are gapped and weakly damped. Close to the SDW QCP, Landau damping takes over and $A(\mathbf{k}_{hs}, \omega)$ has a maximum at $\omega = 0$. This agrees with the recent study by Grossman and Berg [39]. In a generic case when fermionic velocity v_F and bosonic velocity v_s are comparable, pseudogap behavior ends up when the system en-

ters the strong coupling regime near a QCP. If, however, v_s is small compared to v_F , pseudogap behavior extends into the strong coupling regime. We emphasize that this pseudogap is not a precursor to SDW as the magnitude of the pseudogap in $A(\mathbf{k}_{hs}, \omega)$ is set by the mass of the SDW fluctuations, and it must disappear before a QCP.

Pseudogap due to thermal fluctuations We consider a system of fermions, interacting by exchanging spin fluctuations with momentum near \mathbf{Q} . We take as an input that static spin fluctuations have Ornstein-Zernike form with a large, but finite correlation length $\xi = \xi(T)$ and are coupled to fermions by Yukawa coupling \bar{g} , which we assume to be comparable to the bandwidth. Our goal is to obtain the spectral function $A(\mathbf{k}_{hs}, \omega) = -(1/\pi) \text{Im} G_{\text{ret}}(\mathbf{k}_{hs}, \omega)$ for a hot fermion and verify whether at a finite T and large, but still finite ξ , its maximum splits into two maxima at a finite frequency, and whether vertex corrections are crucial for the splitting. For this specific goal, it is sufficient to treat $\xi = \xi(T)$ as an input parameter (for self-consistent calculations of $\xi(T)$ see Refs. [21, 30]).

The spectral function generally can easily obtained by evaluating the thermal self-energy $\Sigma_{\text{th}}(\mathbf{k}_{hs}, \omega)$. We first compute it at the one-loop order, use the result to rationalize the need to include higher-loop contributions, and then analyze $A(\mathbf{k}_{hs}, \omega)$ and the dressed $\Sigma_{\text{th}}(\mathbf{k}_{hs}, \omega)$ with and without vertex corrections.

The one-loop thermal self-energy, shown in Fig. 1 (a), is the convolution of a propagator of a free fermion, $G^{(0)}(\mathbf{k}_{hs} + \mathbf{Q} + \mathbf{q}, \omega)$, and a static spin propagator $\chi(\mathbf{q}) = 1/(\mathbf{q}^2 + \xi^{-2})$. Expanding the fermionic dispersion to linear order in \mathbf{q} and integrating over the two components of \mathbf{q} , one obtains the exact analytical expression [14, 18, 21, 26, 30]

$$\Sigma_{\text{th}}^{(1)}(\mathbf{k}_{hs}, \omega) = v_F \xi^{-1} \lambda_{\text{th}} \times \left[\text{sign}(w) \frac{\log(w + \sqrt{(w)^2 + 1})}{\sqrt{(w)^2 + 1}} - i \frac{\pi}{2\sqrt{(w)^2 + 1}} \right] \quad (1)$$

where $\lambda_{\text{th}} = (3\bar{g}T(2\pi(v_F\xi^{-1})^2))$ is the dimensionless ‘‘thermal’’ coupling, and $w = \omega/(v_F\xi^{-1})$ is the dimensionless frequency. The dimensionless coupling grows as the system approaches the onset temperature T_N of the (π, π) order.

We show the spectral function $A^{(1)}(\mathbf{k}_{hs}, w) = -(1/\pi) \text{Im} \left[\left(v_F \xi^{-1} w - \Sigma_{\text{th}}^{(1)}(\mathbf{k}_{hs}, w) \right)^{-1} \right]$ in Fig. 1 (b). At small λ_{th} , $A^{(1)}(\mathbf{k}_{hs}, w)$ is peaked at $w = 0$, as is expected for a weakly interacting fermion at the Fermi surface. However once λ_{th} exceeds the critical value $\lambda_c = 2\sqrt{2}/(2\sqrt{2} + \pi) \approx 0.4738$, the maximum of $A^{(1)}(\mathbf{k}_{hs}, w)$ shifts to a finite $|w| = \tilde{\Delta}_{\text{pg}} \sim \sqrt{\lambda - \lambda_c}$. The pseudogap

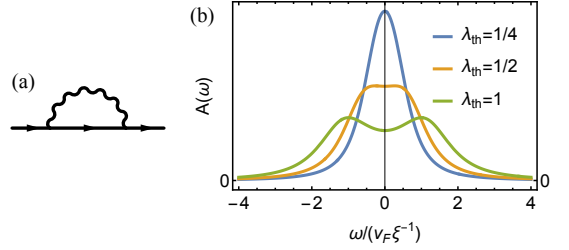


FIG. 1. (a) One-loop self-energy. (b) Spectral function at the hot spot from the one-loop calculation. As the dimensionless coupling $\lambda_{\text{th}} = \frac{3\bar{g}T}{2\pi(v_F\xi^{-1})^2}$ increases, the spectral function shows pseudogap behavior when $\lambda_{\text{th}} > \lambda_c = 0.47$.

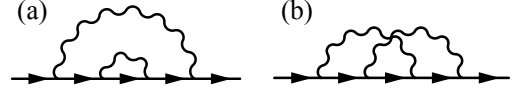


FIG. 2. Non-crossed (a) and crossed (b) two-loop irreducible diagrams.

behavior becomes particularly pronounced at large λ_{th} , where $\tilde{\Delta}_{\text{pg}} > v_F \xi^{-1}$, and at $\omega \sim \tilde{\Delta}_{\text{pg}}$,

$$\int_{\mathbf{q}} G^{(0)}(\mathbf{k}_{hs} + \mathbf{Q} + \mathbf{q}, \omega) \chi(\mathbf{q}) \approx G^{(0)}(\mathbf{k}_{hs} + \mathbf{Q}, \omega) \int_{\mathbf{q}} \chi(\mathbf{q}) \quad (2)$$

such that $\Sigma_{\text{th}}^{(1)}(\mathbf{k}_{hs}, \omega) \approx \tilde{\Delta}_{\text{pg}}^2/\omega$ [14, 18, 21, 26, 30] with $\tilde{\Delta}_{\text{pg}} = (v_F \xi^{-1})(\lambda \log \lambda)^{1/2}/\sqrt{2} \approx \left(\frac{3\bar{g}T}{2\pi} \log \xi \right)^{1/2}$. Here, $\int_{\mathbf{q}} = \int d^2\mathbf{q}$. This self-energy is the same as in the SDW-ordered state, hence the emergence of the peaks at $|\omega| = \tilde{\Delta}_{\text{pg}}$ is quite natural (below the peak, $\text{Im} \Sigma^{(1)}(\mathbf{k}_{hs}, \omega)$ remains non-zero down to the lowest frequencies, hence $\tilde{\Delta}_{\text{pg}}$ is a pseudogap rather than a true gap).

We see that the pseudogap behavior does emerge within the one-loop approximation, however the coupling λ_{th} must exceed $\lambda_c = O(1)$. This raises the question whether the one-loop result stands once we include higher-order terms. Examples of higher-order diagrams for $\Sigma(\mathbf{k}_{hs}, \omega)$ are shown in Fig. 2. They include non-crossed diagrams (Fig. 2 (a)), which account for the renormalization of the internal fermionic line, and crossed diagrams (Fig. 2 (b)), which represent vertex corrections. Besides, the chemical potential μ is different from $\mu_0 = \epsilon_{\mathbf{k}_{hs}}$ and is obtained self-consistently from the condition on the fermionic density. Below we incorporate the change of chemical potential into $\omega \rightarrow \bar{\omega} = \omega + \delta\mu$, where $\delta\mu = \mu - \epsilon_{\mathbf{k}_{hs}} = \mu - \mu_0$.

As a first step, let’s keep only non-crossed higher-loop diagrams, i.e., neglect vertex corrections. The fully dressed self-energy is given by the same one-loop diagram as in the perturbation theory, but with the

fully dressed propagator of an intermediate fermion. This is the SCOLT. The retarded Green's function is $G^{sc}(\mathbf{k}_{hs}, \bar{\omega})^{-1} = v_F \xi^{-1} X$ (sc stand for self-consistent), where $\bar{\omega} = \bar{\omega}/v_F \xi^{-1}$, and $X = X(\bar{\omega})$ is the solution of

$$X = \bar{\omega} - \lambda_{th} \frac{\log(X + \sqrt{X^2 + 1})}{\sqrt{X^2 + 1}} + i\lambda_{th} \frac{\pi}{2\sqrt{X^2 + 1}} \quad (3)$$

Expanding at small $\bar{\omega}$, we find [see Supplementary material (SM) for detail], $X = a\bar{\omega} + ib(1 - c\bar{\omega}^2) + \dots$, where a, b and c are functions of λ_{th} and dots stand for terms of higher order in $\bar{\omega}$. The spectral function $A(\mathbf{k}_{hs}, \bar{\omega}) \propto 1/(b^2 + \bar{\omega}^2(a^2 - b^2c))$. The pseudogap emerges when the prefactor for $\bar{\omega}^2$ is negative, i.e., when $a^2 < b^2c$. We expanded analytically in $\bar{\omega}^2$ and found that this does not happen at any value of λ_{th} : the quasi-particle peak broadens as λ_{th} increases, but remains centered at $\omega = 0$. At large λ_{th} , when $\tilde{\Delta}_{pg} > v_F \xi^{-1}$, the spectral function has a semi-circular form $A^{sc}(\mathbf{k}_{hs}, \bar{\omega}) = \sqrt{4\tilde{\Delta}_{pg}^2 - \bar{\omega}^2}/(2\pi\tilde{\Delta}_{pg}^2)$ at $2\tilde{\Delta}_{pg} > \bar{\omega} > v_F \xi^{-1}$ [14] and remains smooth at $\omega < v_F \xi^{-1}$ as we verified. This spectral function describes incoherent excitations extending up to $2\tilde{\Delta}_{pg}$, and its maximum remains at $\omega = 0$ [40].

We next include the crossed diagrams. We compute the full self-energy directly, by extending perturbation theory to infinite order [41]. The computations again simplify at large λ_{th} , where we can use Eq. (2). Using it for all diagrams, we find that at each loop order the crossed and the non-crossed diagrams are of the same order, and each set forms series in $G^{(0)}(\mathbf{k}_{hs} + \mathbf{Q}, \bar{\omega})G^{(0)}(\mathbf{k}_{hs}, \bar{\omega})\tilde{\Delta}_{pg}^2$. This allows one to keep only one diagram at a given loop order m and multiply it by the proper combinatoric factor \mathcal{D}_m . For the SU(2)-symmetric problem, $\mathcal{D}_m = (2m + 1)!!$ [16, 22]. The full Green's function is then $G^{full}(\mathbf{k}_{hs}, \bar{\omega}) = G^{(0)}(\mathbf{k}_{hs}, \bar{\omega})C(\bar{\omega})$, where

$$C(\bar{\omega}) = \sum_m (2m+1)!! \left(\tilde{\Delta}_{pg}^2 G^{(0)}(\mathbf{k}_{hs}, \bar{\omega}) G^{(0)}(\mathbf{k}_{hs} + \mathbf{Q}, \bar{\omega}) \right)^m \quad (4)$$

Re-expressing the infinite sum as the integral

$$C(\bar{\omega}) = \frac{2}{\sqrt{\pi}} \int_0^\infty dt e^{-t} \frac{t^{1/2}}{1 - ut} \quad (5)$$

where $u = 2\tilde{\Delta}_{pg}^2 G^{(0)}(\mathbf{k}_{hs}, \bar{\omega}) G^{(0)}(\mathbf{k}_{hs} + \mathbf{Q}, \bar{\omega})$, and evaluating it, we obtain for a fermion at a hot spot

$$C(\bar{\omega}) = C(z) = 2z^2 \left(\left(\sqrt{\pi} z e^{-z^2} \text{Erfi}(z) - 1 \right) - i\sqrt{\pi} z e^{-z^2} \right) \quad (6)$$

where $z = \bar{\omega}/(\tilde{\Delta}_{pg}\sqrt{2})$, and $\text{Erfi}(z)$ is the imaginary error

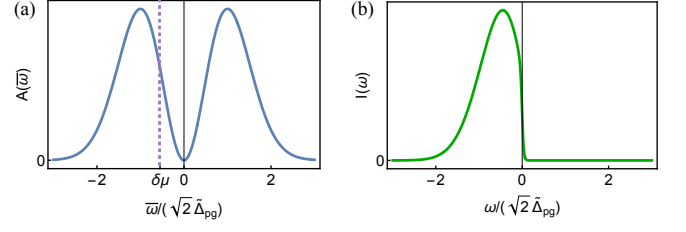


FIG. 3. (a) Spectral function $A^{full}(\mathbf{k}_{hs}, \bar{\omega})$ and (b) Spectral intensity $I^{full}(\mathbf{k}_{hs}, \omega)$ for the SU(2) symmetric model (see Eqs. (7)). The horizontal axis is $\bar{\omega} = \omega + \delta\mu$ in (a) and ω in (b), both in units of $\sqrt{2}\tilde{\Delta}_{pg}$.

function. The spectral function is

$$A^{full}(\mathbf{k}_{hs}, \bar{\omega}) = \frac{1}{\sqrt{2\pi}\tilde{\Delta}_{pg}} \frac{\bar{\omega}^2}{\tilde{\Delta}_{pg}^2} \exp \left[-\frac{\bar{\omega}^2}{2\tilde{\Delta}_{pg}^2} \right] \quad (7)$$

We plot the full spectral function in Fig. 3 (a). We see that it does display the pseudogap behavior. The form of the full $A^{full}(\mathbf{k}_{hs}, \bar{\omega})$ is rather similar to the one-loop result at $\lambda_{th} \gg 1$, and the value of the full pseudogap Δ_{pg} is comparable to $\tilde{\Delta}_{pg}$ [42].

A complimentary way to understand the importance of vertex corrections is to analyze the structure of the thermal self-energy. Dyson equation expresses it in terms of the full Green's function $G^{full}(\mathbf{k}_{hs} + \mathbf{Q}, \bar{\omega})$ and the full vertex $\Gamma(\mathbf{k}_{hs}, \bar{\omega})$ as

$$\Sigma_{th}(\mathbf{k}_{hs}, \bar{\omega}) = 3\tilde{\Delta}_{pg}^2 G^{full}(\mathbf{k}_{hs} + \mathbf{Q}, \bar{\omega}) \Gamma(\mathbf{k}_{hs}, \bar{\omega}). \quad (8)$$

In the SCOLT, $\Gamma(\mathbf{k}_{hs}, \bar{\omega}) = 1$. Using $G^{full} = (G^{(0)} - \Sigma)^{-1}$, we find

$$\Sigma_{th}(\mathbf{k}_{hs}, \bar{\omega}) = \sqrt{2}\tilde{\Delta}_{pg} \bar{\Sigma}(z), \quad \bar{\Sigma}(z) = \frac{z(C(z) - 1)}{C(z)}$$

$$\Gamma(\mathbf{k}_{hs}, \bar{\omega}) = \Gamma(z) = \frac{2}{3} z^2 \frac{C(z) - 1}{C^2(z)} \quad (9)$$

Because $C(z)$ is complex, $\bar{\Sigma}(z)$ and $\Gamma(z)$ are complex functions of the frequency. The spectral function is $A^{full}(\mathbf{k}_{hs}, \bar{\omega}) = A^{full}(z)$, where

$$A^{full}(z) = \left(-\frac{1}{\pi\sqrt{2}\tilde{\Delta}_{pg}} \right) \frac{\text{Im} \bar{\Sigma}(z)}{(z - \text{Re} \bar{\Sigma}(z))^2 + (\text{Im} \bar{\Sigma}(z))^2} \quad (10)$$

We plot real and imaginary parts of $\bar{\Sigma}(z)$ and $\Gamma(z)$ in Fig. 4 (a,b). We see that $\text{Im} \bar{\Sigma}(z)$ is a rather smooth function of z and is featureless around $z = 1$, where the spectral function has a pseudogap peak (see Fig. 3 (a)). On more careful look, we find that the peak in $A^{full}(z)$ at $z = 1$ emerges because $\text{Re} \bar{\Sigma}(z) - z$ changes sign very near $z = 1$ (see Fig. 4 (a)). Further, $\text{Re} \bar{\Sigma}(z) =$

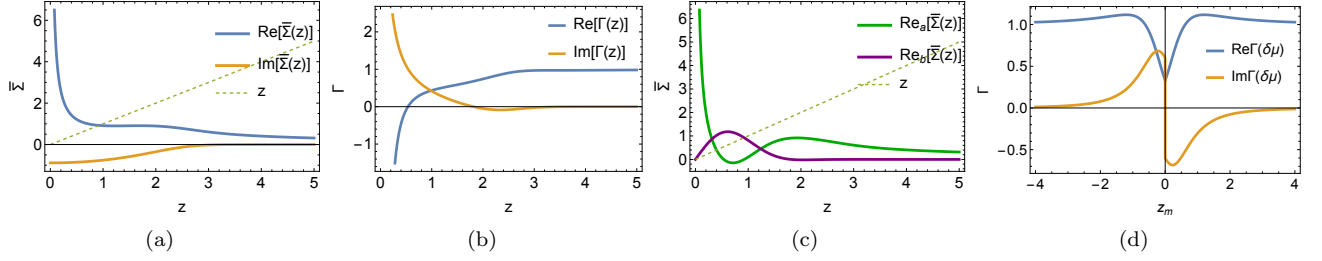


FIG. 4. Panels (a) and (b): real and imaginary part of the normalized self-energy (a) and the vertex function (b) as functions of $z = (\omega + \delta\mu)/(\tilde{\Delta}_{\text{pg}}\sqrt{2})$, from Eq. (9). The the spectral function has a peak at $z \approx 1$, where $\text{Re}\tilde{\Sigma}(z)$ crosses z . Panel (c): two components of $\text{Re}\tilde{\Sigma}(z)$: $\text{Re}_a = (3/2z) = \text{C}(z) \text{Re}\Gamma(z)$ and $\text{Re}_b = -(3/2z) \text{Im}\text{C}(z) \text{Im}\Gamma(z)$. Near $z = 1$, $\text{Re}\tilde{\Sigma}(z) \approx z \approx -(3/2z) \text{Im}\text{C}(z) \text{Im}\Gamma(z)$. Panel (d): $\text{Re}\Gamma(z_m)$ and $\text{Im}\Gamma(z_m)$ along the Matsubara axis at $\delta\mu = -0.8$

$(3/(2z) (\text{Re}\text{C}(z) \text{Re}\Gamma(z) - \text{Im}\text{C}(z) \text{Im}\Gamma(z)))$. We plot the two parts of this expression separately in Fig. 4 (c). We see that near $z = 1$, $\text{Im}\text{C}(z) \text{Im}\Gamma(z) \gg \text{Re}\text{C}(z) \text{Re}\Gamma(z)$. This implies that the imaginary part of the vertex $\Gamma(z)$ is crucial for the pseudogap. One could not obtain the peak in $A^{\text{full}}(z)$ if $\Gamma(z)$ was a constant, like in the SCOLT.

We note in passing that this analysis is different from the one in Refs. [27, 28]. These authors analyzed the vertex function on the Matsubara axis. The latter is complex at a hot spot due to a finite $\delta\mu$, which makes even $G^{(0)}(\mathbf{k}_{\text{hs}}, \omega_m) = 1/(i\omega_m + \delta\mu)$ complex (Refs. [43–45]). In Fig. 4 (d), we plot the real and imaginary parts of $\Gamma(\omega_m)$ for $\delta\mu = 0$ (dashed lines) and $\delta\mu = -0.8$ (solid lines) in unit of $\sqrt{2}\tilde{\Delta}_{\text{pg}}$. We see that $\text{Im}\Gamma(z_m)$ is finite for $\delta\mu \neq 0$. The behavior of $\text{Re}\Gamma(z_m), \text{Im}\Gamma(z_m)$ for $\delta\mu = -0.8$ is quite similar to the vertex function extracted from the numerical analysis of the self-energy in Ref. [27, 28]. At the same time, our results do not support the key point of [27, 28] that the complex structure of $\Gamma(\omega_m)$ on the Matsubara axis is the key to pseudogap development. Indeed, on the real axis, $\delta\mu$ shifts the frequency ω to $\bar{\omega}$, but the two-peak pseudogap behavior emerges independent on the value of $\delta\mu$ and would hold even if $\delta\mu$ was zero [46]. A similar behavior of vertex function Γ in real and imaginary frequency has been observed in Ref. [47] using dynamical mean field theory.

On a more careful look, we found that not all diagrammatic series with both non-crossed and crossed diagrams lead to pseudogap behavior. An example is series with the combinatoric factor $\mathcal{D}_m = (2m - 1)!!$, which holds in certain 1D models [41] and 2D models on a triangular lattice [25]. These series yield $A^{\text{full}}(\mathbf{k}_{\text{hs}}, \omega) \propto \exp(-\bar{\omega}^2/(2\tilde{\Delta}_{\text{pg}}^2))$, which is peaked at $\omega = 0$. For a generic \mathcal{D}_m , the series can be represented as a continued

fraction

$$G^{\text{full}}(\mathbf{k}_{\text{hs}}, i\omega_n) = \frac{1}{i\omega_n - \frac{\kappa_1 \tilde{\Delta}_{\text{pg}}^2}{i\omega_n - \frac{\kappa_2 \tilde{\Delta}_{\text{pg}}^2}{i\omega_n - \frac{\kappa_3 \tilde{\Delta}_{\text{pg}}^2}{i\omega_n - \dots}}}}, \quad (11)$$

We find that for a set of models with $\kappa_j = \kappa^{(0)} + \kappa^{(1)}j$, the spectral function does not show pseudogap behavior. The SCOLT is a member of this set with $\kappa^{(0)} = 1$ and $\kappa^{(1)} = 0$. The case $\kappa^{(0)} = 0, \kappa^{(1)} = 1$ corresponds to $\mathcal{D}_m = (2m - 1)!!$. We verified numerically that for each member of this set, an infinitesimally small deviation $\delta\kappa > 0$ for odd j leads to pseudogap formation (see Fig. 5). For the model with $\kappa_j = \kappa^{(1)}j$ we found analytically

$$A^\kappa(\mathbf{k}_{\text{hs}}, \omega) \propto |\omega|^{2\kappa/\kappa^{(1)}} e^{-\frac{\omega^2}{2\kappa^{(1)}\tilde{\Delta}_{\text{pg}}^2}} \quad (12)$$

This spectral function has two peaks at $|\omega| = \sqrt{\delta\kappa}\tilde{\Delta}_{\text{pg}}$.

That SCOLT is the boundary case for the pseudogap formation can also be seen by analyzing a simple toy model [48, 49], in which the self-energy at large λ is given by

$$\Sigma^{\text{toy}}(\mathbf{k}_{\text{hs}}, \omega) = \tilde{\Delta}_{\text{pg}}^2 \left(\alpha G(\mathbf{k}_{\text{hs}}, \omega) + (1 - \alpha) G^{(0)}(\mathbf{k}_{\text{hs}}, \omega) \right) \quad (13)$$

where $0 \leq \alpha \leq 1$. This self-energy interpolates between perturbative one-loop theory at $\alpha = 0$ and SCOLT at $\alpha = 1$. The spectral function $A^{\text{toy}}(\mathbf{k}_{\text{hs}}, \omega)$ is readily obtained by solving the self-consistent equation for the Green's function $G^{-1}(\mathbf{k}_{\text{hs}}, \omega) = \omega - \tilde{\Delta}_{\text{pg}}^2 (\alpha G(\mathbf{k}_{\text{hs}}, \omega) + (1 - \alpha) G^{(0)}(\mathbf{k}_{\text{hs}}, \omega))$ [see SM for detail]. For any $\alpha < 1$, the maximum of $A^{\text{toy}}(\mathbf{k}_{\text{hs}}, \omega)$ is at a finite $|\omega| = \tilde{\Delta}_{\text{pg}}(1 - \alpha)^{1/2}$, at $\alpha = 1$ it is at $\omega = 0$. We again see that the SCOLT is the boundary case for the pseudogap formation.

Pseudogap from quantum fluctuations. We argued above that thermal spin fluctuations give rise to pseudogap behavior as a precursor to the (π, π) ordered

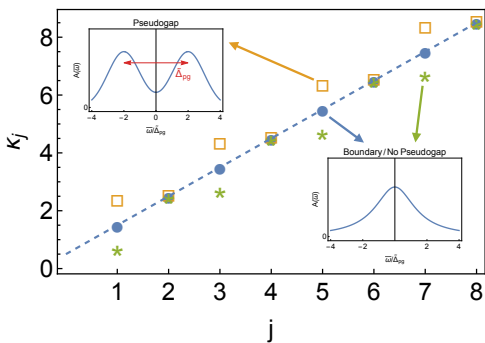


FIG. 5. Illustration that the set of models with $\kappa_j = \kappa^{(0)} + \kappa^{(1)}j$ (see Eq. (11)) are at the boundary of the pseudogap formation. The boundary models from the set are along the solid line. We verified that the pseudogap emerges at infinitesimally small $\delta k > 0$ at odd j (orange square).

state. We now contrast this behavior with the one at $T = 0$. We neglect superconductivity and analyze whether quantum spin fluctuations can give rise to the pseudogap.

We use the same model as before, but with the dynamical spin propagator $\chi(\mathbf{q}, \Omega_m) = \chi_0 / ((\Omega_m/v_s)^2 + (\mathbf{q} - \mathbf{Q})^2 + \xi^{-2} + \gamma|\Omega_m|)$, where v_s is spin velocity and the last term is the Landau damping with $\gamma = (4/\pi \sin \theta)\bar{g}/v_F^2$, where θ is the angle between Fermi velocities at \mathbf{k}_{hs} and $\mathbf{k}_{hs} + \mathbf{Q}$ [50]. We restrict with perturbative one-loop analysis as higher-loop terms at $T = 0$ are at most $O(1)$ relative to the one-loop term [50]. The exact one-loop self-energy can be readily obtained (see SM for detail), and its analysis shows that at small $\lambda_q = 3\bar{g}/(4\pi v_F \xi^{-1})$, the spectral function $A^q(\mathbf{k}_{hs}, \omega)$ nearly vanishes at $|\omega| < v_s \xi^{-1}$ and has a peak at $|\omega| \geq v_s \xi^{-1}$. In the opposite limit of large λ_q , the Landau damping term is the strongest one in the spin propagator, and $A^q(\mathbf{k}_{hs}, \omega)$ has a broad peak centered at $\omega = 0$. In both cases, the spectral function also has a δ -functional peak at $\omega = 0$, with overall intensity proportional to the quasiparticle residue [39] [51].

We analyzed the evolution of the spectral function with increasing λ_q at various $\alpha_v = v_F/v_s$ and found self-consistently critical λ_q^{cr} , at which pseudogap behavior at $T = 0$ disappears. We show the results in Fig. 6. For generic $\alpha_v = O(1)$, $\lambda_q^{cr} = O(1)$, i.e., there is no pseudogap in the strong coupling regime. The situation changes when $v_s \ll v_F$, i.e., α_v is large. In this limit, we find analytically $\lambda_q^{cr} = c\alpha_v$, where $c \approx (3 \sin \theta/16)\sqrt{10/3}$. Still, at large enough ξ , $\lambda_q > \lambda_q^{cr}$, which implies that near a QCP the one-loop spectral function does not display pseudogap behavior at $T = 0$. In other words, pseudogap behavior at $T = 0$ is *not* a precursor to SDW [52].

Summary. Previous works have found that in a metal, whose ground state is antiferromagnetically ordered with $\mathbf{Q} = (\pi, \pi)$ thermal magnetic fluctuations give

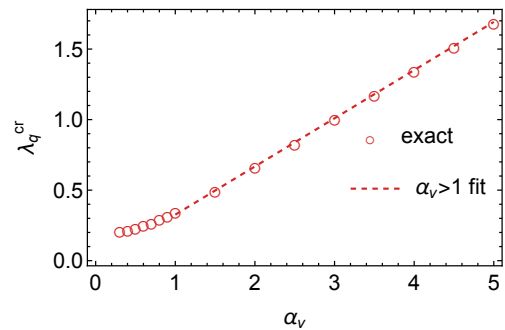


FIG. 6. Critical λ_q at different $\alpha_v = v_F/v_s$ and $\theta = \pi/2$, i.e. $\gamma = 4\bar{g}/(\pi v_F^2)$. The spectral function shows pseudogap behavior for $\lambda_q < \lambda_q^{cr}$. Red circles are λ_q^{cr} , extracted from the exact formula for the one-loop self-energy, and dashed line in the linear fit by $\lambda_q^{cr} = 0.085 + c\alpha_v$ with the same prefactor for α_v that we obtained analytically in the $\alpha_v \gg 1$ limit (see the text).

rise to pseudogap behavior in some temperature range above T_N , when the spectral function of a hot fermion contains two peaks, separated by roughly the same energy as in the antiferromagnetically ordered state. This behavior has been obtained theoretically by departing from free fermions in a paramagnet and evaluating the dressed fermionic Green's function by summing up infinite series of non-crossed and crossed diagrams for the fermionic Green's function. The crossed diagrams describe vertex corrections. We show that keeping vertex corrections is crucial as the combined contribution from non-crossed diagrams broadens the spectral function of a hot fermion, but keeps its maximum at zero frequency. We argue therefore that to capture the physics of a magnetic pseudogap, one has to go beyond self-consistent one-loop theories, like, e.g., Eliashberg theory for superconductivity. This result is relevant for the understanding of the observed reduction of superconducting T_c when superconductivity comes out of a pseudogap phase, as within the Eliashberg theory thermal fluctuations do not affect T_c . We expect that similar results hold for incommensurate spin fluctuations.

We also analyzed potential pseudogap behavior at $T = 0$, due to quantum fluctuations, assuming no superconductivity. We found that pseudogap may exist at a finite correlation length ξ and may even extend into the strong coupling regime. Still, this pseudogap behavior is not the precursor to the ordered state but rather the consequence of the fact that when spin fluctuations are weakly damped propagating massive bosons, the spectral function of a hot fermion is strongly reduced below the threshold set by the bosonic mass. We found that sufficiently close to an antiferromagnetic QCP, the spectral function of a hot fermion does not display pseudogap behavior at $T = 0$. Combining this with the result of our

earlier work [30] that thermal fluctuations do not give rise to pseudogap behavior when the ground state is not ordered, we conclude that when the ground state is not magnetically ordered, there is no magnetic pseudogap at any T due to long-range magnetic fluctuations. A potential pseudogap due to short-range fluctuations in a doped Mott insulator has been analyzed in [53].

ACKNOWLEDGMENTS

We thank Leon Balents, Erez Berg, Rafael Fernandes, Antoine Georges, Patrick Lee, Izabella Lovas,

Michael Sadovskii, Subir Sachdev, Jörg Schmalian, Fedor Simkovic, and particularly André-Marie Tremblay for helpful discussions and suggestions. M.Y. was supported by the Gordon and Betty Moore Foundation through Grant GBMF8690 to UCSB, by a grant from the Simons Foundation (216179, LB), and by the National Science Foundation under Grant No. NSF PHY-1748958. AVC was supported by the U.S. Department of Energy, Office of Science, Basic Energy Sciences, under Award No. DE-SC0014402.

-
- [1] M. A. Metlitski and S. Sachdev, Quantum phase transitions of metals in two spatial dimensions. ii. spin density wave order, *Phys. Rev. B* **82**, 075128 (2010).
 - [2] Y. Wang and A. Chubukov, Charge-density-wave order with momentum $(2q, 0)$ and $(0, 2q)$ within the spin-fermion model: Continuous and discrete symmetry breaking, preemptive composite order, and relation to pseudogap in hole-doped cuprates, *Phys. Rev. B* **90**, 035149 (2014).
 - [3] D. Chowdhury and S. Sachdev, Feedback of superconducting fluctuations on charge order in the underdoped cuprates, *Phys. Rev. B* **90**, 134516 (2014).
 - [4] W. A. Atkinson, A. P. Kampf, and S. Bulut, Charge order in the pseudogap phase of cuprate superconductors, *New Journal of Physics* **17**, 013025 (2015).
 - [5] R. Arpaia, S. Caprara, R. Fumagalli, G. D. Vecchi, Y. Y. Peng, E. Andersson, D. Betto, G. M. D. Luca, N. B. Brookes, F. Lombardi, M. Salluzzo, L. Braicovich, C. D. Castro, M. Grilli, and G. Ghiringhelli, Dynamical charge density fluctuations pervading the phase diagram of a Cu-based high- T_c superconductor, *Science* **365**, 906 (2019).
 - [6] C. M. Varma, Non-fermi-liquid states and pairing instability of a general model of copper oxide metals, *Phys. Rev. B* **55**, 14554 (1997).
 - [7] C. M. Varma, Pseudogap phase and the quantum-critical point in copper-oxide metals, *Phys. Rev. Lett.* **83**, 3538 (1999).
 - [8] S. Sachdev, H. D. Scammell, M. S. Scheurer, and G. Tarnopolsky, Gauge theory for the cuprates near optimal doping, *Physical Review B* **99**, 10.1103/physrevb.99.054516 (2019).
 - [9] Y.-H. Zhang and S. Sachdev, From the pseudogap metal to the fermi liquid using ancilla qubits, *Phys. Rev. Res.* **2**, 023172 (2020).
 - [10] E. Mascot, A. Nikolaenko, M. Tikhonovskaya, Y.-H. Zhang, D. K. Morr, and S. Sachdev, Electronic spectra with paramagnon fractionalization in the single-band hubbard model, *Phys. Rev. B* **105**, 075146 (2022).
 - [11] A. Nikolaenko, J. von Milczewski, D. G. Joshi, and S. Sachdev, Spin density wave, fermi liquid, and fractionalized phases in a theory of antiferromagnetic metals using paramagnons and bosonic spinons, *Phys. Rev. B* **108**, 045123 (2023).
 - [12] M. Christos, Z.-X. Luo, H. Shackleton, Y.-H. Zhang, M. S. Scheurer, and S. Sachdev, A model of d -wave superconductivity, antiferromagnetism, and charge order on the square lattice, *Proceedings of the National Academy of Sciences* **120**, e2302701120 (2023).
 - [13] Y. M. Vilks and A. M. S. Tremblay, Destruction of fermi-liquid quasiparticles in two dimensions by critical fluctuations, *Europhysics Letters* **33**, 159 (1996).
 - [14] Y.M. Vilks and A.-M.S. Tremblay, Non-perturbative many-body approach to the hubbard model and single-particle pseudogap, *J. Phys. I France* **7**, 1309 (1997).
 - [15] J. Schmalian, D. Pines, and B. Stojković, Weak pseudogap behavior in the underdoped cuprate superconductors, *Phys. Rev. Lett.* **80**, 3839 (1998).
 - [16] J. Schmalian, D. Pines, and B. Stojković, Microscopic theory of weak pseudogap behavior in the underdoped cuprate superconductors: General theory and quasiparticle properties, *Phys. Rev. B* **60**, 667 (1999).
 - [17] É. Z. Kuchinskii and M. V. Sadovskii, Models of the pseudogap state of two-dimensional systems, *Journal of Experimental and Theoretical Physics* **88**, 968 (1999).
 - [18] C. P. Moca, I. Tifrea, and M. Crisan, An analytical approach for the pseudogap in the spin fluctuations model, *Journal of Superconductivity* **13**, 411 (2000).
 - [19] M. V. Sadovskii, Pseudogap in high-temperature superconductors, *Phys. Usp.* **44**, 515 (2001).
 - [20] Y. Yanase, Pseudogap and superconducting fluctuation in high- T_c cuprates: Theory beyond 1-loop approximation, *Journal of the Physical Society of Japan* **73**, 1000 (2004), <https://doi.org/10.1143/JPSJ.73.1000>.
 - [21] S. Roy and A.-M. S. Tremblay, Scaling and commensurate-incommensurate crossover for the $d=2$, $z=2$ quantum critical point of itinerant antiferromagnets, *Europhysics Letters* **84**, 37013 (2008).
 - [22] T. A. Sedrakyants and A. V. Chubukov, Pseudogap in underdoped cuprates and spin-density-wave fluctuations, *Phys. Rev. B* **81**, 174536 (2010).

- [23] J. P. F. LeBlanc, A. E. Antipov, F. Becca, I. W. Bulik, G. K.-L. Chan, C.-M. Chung, Y. Deng, M. Ferrero, T. M. Henderson, C. A. Jiménez-Hoyos, E. Kozik, X.-W. Liu, A. J. Millis, N. V. Prokof'ev, M. Qin, G. E. Scuseria, H. Shi, B. V. Svistunov, L. F. Tocchio, I. S. Tupitsyn, S. R. White, S. Zhang, B.-X. Zheng, Z. Zhu, and E. Gull (Simons Collaboration on the Many-Electron Problem), Solutions of the two-dimensional hubbard model: Benchmarks and results from a wide range of numerical algorithms, *Phys. Rev. X* **5**, 041041 (2015).
- [24] O. Gunnarsson, T. Schäfer, J. P. F. LeBlanc, E. Gull, J. Merino, G. Sangiovanni, G. Rohringer, and A. Toschi, Fluctuation diagnostics of the electron self-energy: Origin of the pseudogap physics, *Phys. Rev. Lett.* **114**, 236402 (2015).
- [25] M. Ye and A. V. Chubukov, Hubbard model on a triangular lattice: Pseudogap due to spin density wave fluctuations, *Phys. Rev. B* **100**, 035135 (2019).
- [26] T. Schäfer, N. Wentzell, F. Šimkovic, Y.-Y. He, C. Hille, M. Klett, C. J. Eckhardt, B. Arzhang, V. Harkov, F. m. c.-M. Le Régent, A. Kirsch, Y. Wang, A. J. Kim, E. Kozik, E. A. Stepanov, A. Kauch, S. Andergassen, P. Hansmann, D. Rohe, Y. M. Vilk, J. P. F. LeBlanc, S. Zhang, A.-M. S. Tremblay, M. Ferrero, O. Parcollet, and A. Georges, Tracking the footprints of spin fluctuations: A multimethod, multimessenger study of the two-dimensional hubbard model, *Phys. Rev. X* **11**, 011058 (2021).
- [27] *Beyond DMFT: Spin Fluctuations, Pseudogaps and Superconductivity* (2022) [arXiv:2208.03174](https://arxiv.org/abs/2208.03174) [cond-mat.str-el].
- [28] F. Krien, P. Worm, P. Chalupa, A. Toschi, and K. Held, Spin scattering turns complex at strong coupling: the key to pseudogap and fermi arcs in the hubbard model (2021), [arXiv:2107.06529](https://arxiv.org/abs/2107.06529) [cond-mat.str-el].
- [29] IV, Fedor Šimkovic and Rossi, Riccardo and Ferrero, Michel, Two-dimensional hubbard model at finite temperature: Weak, strong, and long correlation regimes, *Phys. Rev. Res.* **4**, 043201 (2022); F. Simkovic, R. Rossi, A. Georges, and M. Ferrero, Origin and fate of the pseudogap in the doped hubbard model (2022), [arXiv:2209.09237](https://arxiv.org/abs/2209.09237) [cond-mat.str-el].
- [30] M. Ye, Z. Wang, R. M. Fernandes, and A. V. Chubukov, Location and thermal evolution of the pseudogap due to spin fluctuations (2023), [arXiv:2304.08623](https://arxiv.org/abs/2304.08623) [cond-mat.str-el].
- [31] M. R. Norman, M. Randeria, H. Ding, and J. C. Campuzano, Phenomenology of the low-energy spectral function in high- T_c superconductors, *Phys. Rev. B* **57**, R11093 (1998).
- [32] M. Franz and A. J. Millis, Phase fluctuations and spectral properties of underdoped cuprates, *Phys. Rev. B* **58**, 14572 (1998).
- [33] S. Fujimoto, Pseudogap phenomena in the bcs pairing model, *Journal of the Physical Society of Japan* **71**, 1230 (2002), <https://doi.org/10.1143/JPSJ.71.1230>.
- [34] E. Berg and E. Altman, Evolution of the fermi surface of d -wave superconductors in the presence of thermal phase fluctuations, *Phys. Rev. Lett.* **99**, 247001 (2007).
- [35] Y.-M. Wu, S.-S. Zhang, A. Abanov, and A. V. Chubukov, Interplay between superconductivity and non-fermi liquid behavior at a quantum-critical point in a metal. v. the γ model and its phase diagram: The case $\gamma = 2$, *Phys. Rev. B* **103**, 184508 (2021).
- [36] Z. Dai and P. A. Lee, Superconductinglike response in a driven gapped bosonic system, *Phys. Rev. B* **104**, 054512 (2021).
- [37] X.-C. Wang and Y. Qi, Phase fluctuations in two-dimensional superconductors and pseudogap phenomenon, *Phys. Rev. B* **107**, 224502 (2023).
- [38] Z. Dai, T. Senthil, and P. A. Lee, Modeling the pseudogap metallic state in cuprates: Quantum disordered pair density wave, *Phys. Rev. B* **101**, 064502 (2020).
- [39] O. Grossman and E. Berg, Weakly damped bosons and precursor gap in the vicinity of an antiferromagnetic metallic transition (2023), [arXiv:2304.12697](https://arxiv.org/abs/2304.12697) [cond-mat.str-el].
- [40] We note in passing that the total spectral weight is the same as in $A^{(1)}(\mathbf{k}_{hs}, \bar{\omega})$, where at such λ_{th} it is concentrated around the near- δ - functional peaks at $|\bar{\omega}| = \tilde{\Delta}_{pg}$.
- [41] M. V. Sadovskii, A model of a disordered system (A contribution to the theory of "liquid semiconductors"), *Soviet Journal of Experimental and Theoretical Physics* **39**, 845 (1974); Theory of quasi-one-dimensional systems undergoing peierls transition, *Sov. Phys. -Solid State* v.16, 1632 (1974); Exact solution for the density of electronic states in a model of a disordered system, *Zh. Eksp. Theor. Fiz.* **77**, 2070 (1979) [*Sov. Phys. JETP* **50**, 989 (1979)] (1979); Sadovskii, M. V., *Diagrammatics: Lectures on Selected Problems in Condensed Matter Theory* (World Scientific Publishing Co, 2006).
- [42] We note in passing that within SCOLT, the Green's function can also be represented as an infinite sum of multi-loop diagrams, like in Eq. (4), but with the combinatoric factor $\mathcal{D}_m = 2^{2m+1}(2m-1)!!/(2m+2)!!$. Solving Eq. (4) with this \mathcal{D}_m , we reproduce the spectral function solution $A^{(sc)}(\mathbf{k}_{hs}, \bar{\omega}) \propto \sqrt{4\tilde{\Delta}_{pg}^2 - \bar{\omega}^2}$.
- [43] Y. Gu, A. Kitaev, S. Sachdev, and G. Tarnopolsky, Notes on the complex sachdev-ye-kitaev model, *Journal of High Energy Physics* **2020**, 157 (2020).
- [44] A. Georges, O. Parcollet, and S. Sachdev, Quantum fluctuations of a nearly critical heisenberg spin glass, *Phys. Rev. B* **63**, 134406 (2001).
- [45] Y. Wang and A. V. Chubukov, Quantum phase transition in the yukawa-syk model, *Phys. Rev. Res.* **2**, 033084 (2020).
- [46] A finite negative $\delta\mu$ relates the observable photoemission intensity $I(\mathbf{k}_{hs}, \omega) = A^{full}(\mathbf{k}_{hs}, \omega)n_F(\omega)$ to the behavior of $A^{full}(\mathbf{k}_{hs}, \bar{\omega})$ at negative $\bar{\omega}$, subject to $\bar{\omega} < -|\delta\mu|$. Because of this constraint, the singular behavior of $\Sigma_{th}(z)$ and $\Gamma(z)$ at $z \rightarrow 0$ (Fig. 4d) is not accessible in photoemission experiments.
- [47] E. G. C. P. van Loon, F. Krien, H. Hafermann, A. I. Lichtenstein, and M. I. Katsnelson, Fermion-boson vertex within dynamical mean-field theory, *Phys. Rev. B* **98**,

205148 (2018).

- [48] A. I. Posazhennikova and M. V. Sadovskii, The ginzburg-landau expansion in the simple model of a superconductor with a pseudogap, *Journal of Experimental and Theoretical Physics* **88**, 347 (1999).
- [49] E. Z. Kuchinskii and M. V. Sadovskii, Superconductivity in a simple model of the pseudogap state, *Journal of Experimental and Theoretical Physics* **90**, 535 (2000).
- [50] A. Abanov, A. V. Chubukov, and J. Schmalian, Quantum-critical theory of the spin-fermion model and its application to cuprates: Normal state analysis, *Advances in Physics* **52**, 119 (2003), <https://doi.org/10.1080/0001873021000057123>.
- [51] This δ -function is obtained by either adding $i0$ to ω (this corresponds to treating $T = 0$ as the limit $T \rightarrow 0$ and using the fact that at any finite T , $\text{Im } \Sigma(\mathbf{k}, 0)$ is finite), or by evaluating $A^q(\mathbf{k}, \omega)$ at \mathbf{k} , for which $\epsilon_{\mathbf{k}+\mathbf{Q}}$ is finite, and taking the limit $\mathbf{k} \rightarrow \mathbf{k}_{h.s.}$.
- [52] In principle, there may be another possibility to suppress the Landau damping even without requiring $v_s \ll v_F$. Namely, if one *assumes* that the pseudogap exists and evaluate γ using the Green's functions with the pseudogap, one find that γ indeed gets reduced. We don't know, however, whether such a state can be ever reached by approaching a QCP from the paramagnetic state.
- [53] D. Sénéchal and A.-M. S. Tremblay, Hot spots and pseudogaps for hole- and electron-doped high-temperature superconductors, *Phys. Rev. Lett.* **92**, 126401 (2004).

SUPPLEMENTAL MATERIAL

A: DETAILS OF SELF-CONSISTENT ONE-LOOP THEORY

In this section, we show that the pseudogap behavior does not develop in the self-consistent one-loop theory (SCOLT) for any λ_{th} .

The spectral function in SCOLT is $G^{sc}(\mathbf{k}_{\text{hs}}, \bar{\omega})^{-1} = v_F \xi^{-1} X$, where $\bar{\omega} = \bar{\omega}/v_F \xi^{-1}$, and $X = X(\bar{\omega})$ is the solution of

$$X = \bar{\omega} - \lambda_{\text{th}} \frac{\log(X + \sqrt{X^2 + 1})}{\sqrt{X^2 + 1}} + i\lambda_{\text{th}} \frac{\pi}{2\sqrt{X^2 + 1}} \quad (14)$$

(see the main text). A way to see whether pseudogap behavior develops is to expand the spectral function $A(\omega) = (1/\pi)|\text{Im} G(\omega)|$ at small ω as $A(\omega) = A(0)(1 - d\omega^2)$ and check the sign of d . Pseudogap develops when d is negative.

Expanding $X(\bar{\omega})$ at small $\bar{\omega}$, we find $X = a\bar{\omega} + ib(1 - c\bar{\omega}^2) + \dots$, where dots stand for higher-order terms that do not contribute to d . Solving self-consistently for a, b , and c , we find after tedious but straightforward algebra the set of equations

$$\begin{aligned} b\sqrt{1 - b^2} &= \lambda_{\text{th}} \left(\frac{\pi}{2} + i \log ib + \sqrt{1 - b^2} \right) \\ a &= 1 + \frac{a}{1 - b^2} (\lambda_{\text{th}} - b^2) \\ c &= \frac{a^2}{2(1 - b^2)} \frac{1 + 2b^2 - 3\lambda_{\text{th}}}{1 - 2b^2 + \lambda_{\text{th}}} \end{aligned} \quad (15)$$

These equations are valid for $b < 1$, which holds for $\lambda_{\text{th}} < 1$, as we find a posteriori.

Evaluating $A(\bar{\omega}) \propto \text{Im} X^{-1}(\bar{\omega})$, we find

$$d = d_0 \left(1 - \frac{b^2 c}{a^2} \right) \quad (16)$$

where $d_0 > 0$. Hence the sign of d is the same as of

$$1 - \frac{b^2 c}{a^2} = 1 - \frac{b^2(1 + 2b^2 - 3\lambda_{\text{th}})}{2(1 - b^2)(1 - 2b^2 + \lambda_{\text{th}})} \quad (17)$$

where b is determined from (15). Expressing $b = \cos \psi$, $\sqrt{1 - b^2} = \sin \psi$, such that $\psi = \pi/2$ at $b = 0$ and $\psi \rightarrow 0$ at $b \rightarrow 1$, we obtain from (15),

$$2\lambda_{\text{th}}\psi = \sin 2\psi \quad (18)$$

and

$$1 - \frac{b^2 c}{a^2} = 1 - \frac{\cos^2 \phi}{2 \sin \phi} \frac{2 + \cos 2\phi - 3\lambda_{\text{th}}}{\lambda_{\text{th}} - \cos 2\psi} \quad (19)$$

Solving (18) for $\psi = \psi(\lambda_{\text{th}})$ and substituting into (19), we find that $1 - b^2 c/a^2$ remains positive for all $\lambda_{\text{th}} < 1$. At $\lambda_{\text{th}} \rightarrow 0$, $1 - b^2 c/a^2 \rightarrow 1$, at $\lambda_{\text{th}} \rightarrow 1$, $1 - b^2 c/a^2 \rightarrow 0.9$.

For $\lambda_{\text{th}} > 1$, similar analysis yields

$$1 - \frac{b^2 c}{a^2} = 1 - \frac{b^2(1 + 2b^2 - 3\lambda_{\text{th}})}{2(b^2 - 1)(2b^2 - 1 - \lambda_{\text{th}})} \quad (20)$$

where b is determined by

$$b\sqrt{b^2 - 1} = \lambda_{\text{th}} \log b + \sqrt{b^2 - 1} \quad (21)$$

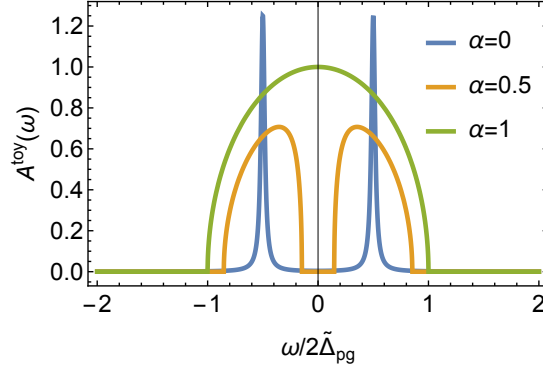


FIG. 7. Electron spectral function from the toy model of Eq. (24).

Introducing $b = \cosh \psi$ and $\sqrt{b^2 - 1} = \sinh \psi$ such that $\psi = 0+$ at $b = 1 + 0$ and $\psi \approx \log 2b$ at $b \gg 1$, we rewrite (20) and (21) as

$$\sinh 2\psi = 2\lambda_{\text{th}}\psi \quad (22)$$

$$1 - \frac{b^2 c}{a^2} = 1 - \frac{\coth^2 \psi}{2} \frac{1 + 2 \cosh^2 \psi - 3\lambda_{\text{th}}}{2 \cosh^2 \psi - 1 - \lambda_{\text{th}}} \quad (23)$$

Solving (22) for $\psi = \psi(\lambda_{\text{th}})$ and substituting into (20), we obtain that $1 - b^2 c/a^2$ remains positive. Hence, $d \propto (1 - b^2 c/a^2)$ is positive for all λ_{th} . A positive d implies that the spectral function has a maximum at $\omega = 0$, hence pseudogap behavior does not develop.

B: TOY MODELS

In the section, we discuss two toy models for the pseudogap, which both interpolate between SCOLT and perturbative one-loop theory.

First, we consider the toy model introduced in the main text (Eq. (13)). Within this model, the self-energy at large λ_{th} is given by

$$\Sigma^{\text{toy1}}(\mathbf{k}_{\text{hs}}, \omega) = \tilde{\Delta}_{\text{pg}}^2 \left(\alpha G(\mathbf{k}_{\text{hs}}, \omega) + (1 - \alpha) G^{(0)}(\mathbf{k}_{\text{hs}}, \omega) \right) \quad (24)$$

where $0 \leq \alpha \leq 1$. This self-energy interpolates between perturbative one-loop theory at $\alpha = 0$ and SCOLT at $\alpha = 1$. The spectral function $A^{\text{toy}}(\mathbf{k}_{\text{hs}}, \omega)$ is readily obtained by solving the self-consistent equation for the Green's function $G^{-1}(\mathbf{k}_{\text{hs}}, \omega) = \omega - \tilde{\Delta}_{\text{pg}}^2 (\alpha G(\mathbf{k}_{\text{hs}}, \omega) + (1 - \alpha) G^{(0)}(\mathbf{k}_{\text{hs}}, \omega))$ and is shown in Fig. 7. $A^{\text{toy1}}(\mathbf{k}_{\text{hs}}, \omega)$ is non-zero in a finite range between $|\omega_{\text{min}}| = \tilde{\Delta}_{\text{pg}}(1 - \sqrt{\alpha})$ and $|\omega_{\text{max}}| = \tilde{\Delta}_{\text{pg}}(1 + \sqrt{\alpha})$. The maxima are at $|\omega| = \tilde{\Delta}_{\text{pg}}(1 - \alpha)^{1/2}$, which remains finite as long as $\alpha < 1$. In particular, for $\alpha = 0$, $A^{\text{toy1}}(\mathbf{k}_{\text{hs}}, \omega)$ has δ -functional peaks at $\omega = \pm \tilde{\Delta}_{\text{pg}}$. For $\alpha = 1$ (SCOLT), it is a semi-circle at $|\omega| < 2\tilde{\Delta}_{\text{pg}}$ with the maximum at $\omega = 0$, and there is no pseudogap. We see that the SCOLT is the boundary case for the pseudogap formation.

Another way to interpolate between the one-loop perturbation theory and SCOLT is to consider the self-energy at a hot spot in the form

$$\Sigma^{\text{toy2}}(\omega) = \frac{\tilde{\Delta}_{\text{pg}}^2}{\omega - \alpha \Sigma^{\text{toy2}}(\omega)} \quad (25)$$

where $\tilde{\Delta}_{\text{pg}} = (v_F \xi^{-1})(\lambda_{\text{th}} \log \lambda_{\text{th}})^{1/2} / \sqrt{2} \approx \left(\frac{3gT}{2\pi} \log \xi \right)^{1/2}$ is the same as in the main text. At $\alpha = 0$, $\Sigma^{\text{toy2}}(\omega)$ is the same as in the one-loop perturbation theory, and the spectral function has two δ -functional peaks at $\omega = \pm \tilde{\Delta}_{\text{pg}}$.

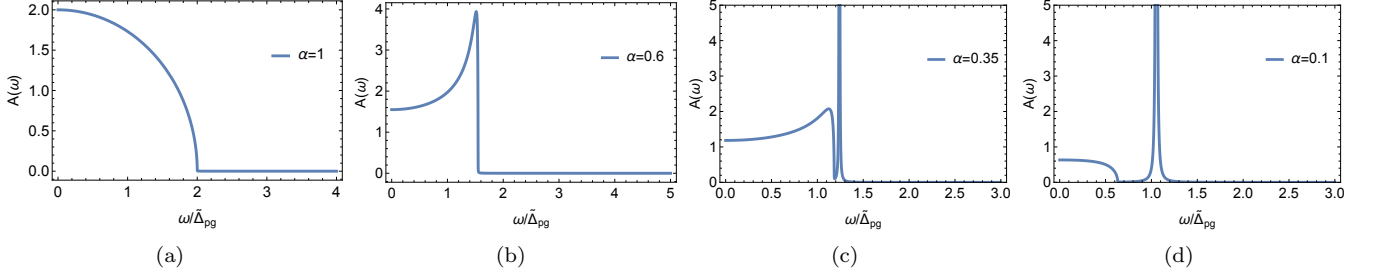


FIG. 8. Spectral function at different α for the toy model Eq. (26). Pseudogap develops for $\alpha < \alpha_{cr,1} = 0.854$.

At $\alpha = 1$, $\Sigma^{\text{toy2}}(\omega)$ is the same as in the SCOLT, and the spectral function $A^{\text{toy2}}(\omega) \propto \sqrt{4\tilde{\Delta}_{\text{pg}}^2 - \omega^2}$, with the maximum at $\omega = 0$.

The analysis at intermediate α is straightforward, one just has to solve the quadratic equation for $\Sigma^{\text{toy2}}(\omega)$ and substitute the result into the spectral function. We depart from $\alpha = 1$ and gradually decrease α .

For the retarded fermionic Green's function at a hot spot we obtain for $\omega > 0$,

$$G^{\text{toy2}}(\omega) = \frac{2\alpha}{\omega(2\alpha - 1) + \sqrt{\omega^2 - 4\tilde{\Delta}_{\text{pg}}^2\alpha} + i0}. \quad (26)$$

A way to check whether pseudogap develops is to expand the spectral function $A^{\text{toy2}}(\omega) = (1/\pi)|\text{Im}G(\omega)|$ near $\omega = 0$ and check the sign of the slope. Expanding to order ω^2 , we obtain

$$A^{\text{toy2}}(\omega) = \frac{\sqrt{\alpha}}{\pi\tilde{\Delta}_{\text{pg}}} \left(1 - \frac{\omega^2}{8\tilde{\Delta}_{\text{pg}}^2\alpha} (1 - 8\alpha + 8\alpha^2) \right) + O(\omega^4) \quad (27)$$

The maximum of $A^{\text{toy2}}(\omega)$ is at $\omega = 0$ at $\alpha = 1$, and an elementary analysis shows that this holds at $\alpha > \alpha_{cr,1} = (1 + 1/\sqrt{2})/2 = 0.854$. For these α , the maximum of $A^{\text{toy2}}(\omega)$ remains at $\omega = 0$, as in SCOLT. At smaller α , the maximum shifts to finite ω , i.e., the spectral function develops a pseudogap behavior. We show this in panels (a) and (b) of Fig. 8.

This behavior holds at $\alpha > 1/2$. At smaller α , the spectral function develops a δ -functional peak at $\omega = \tilde{\Delta}_{\text{pg}}/\sqrt{1 - \alpha}$ (Fig. 8 (c)). The spectral function at these α consists of a δ -function and a continuum at $\omega < 2\tilde{\Delta}_{\text{pg}}\sqrt{\alpha}$. The spectral function in the continuum remains peaked at a finite ω down to $\alpha_{cr,2} = (1 - 1/\sqrt{2})/2 = 0.146$. At $\alpha < \alpha_{cr,2}$, the continuum part of $A^{\text{toy2}}(\omega)$ is peaked at $\omega = 0$ (Fig. 8 (d)). Finally, at $\alpha = 0$, the continuum disappears, and $A^{\text{toy2}}(\omega)$ only has a δ -functional peak at $\omega = \tilde{\Delta}_{\text{pg}}$, as in the perturbative one-loop theory.

C: SELF-ENERGY AT $T = 0$.

We use the model of fermions with $t - t'$ dispersion, coupled by Yukawa \bar{g} to dressed dynamical spin fluctuations with the propagator (in Matsubara frequencies) $\chi(\mathbf{q}, \Omega_m) = \chi_0 / ((\Omega_m/v_s)^2 + (\mathbf{q} - \mathbf{Q})^2 + \xi^{-2} + \gamma|\Omega_m|)$, where v_s is spin velocity, $\mathbf{Q} = (\pi, \pi)$, and the Landau damping term $\gamma|\Omega_m|$ comes from inserting particle-hole bubbles into the spin propagator using the same Yukawa spin-fermion coupling. The prefactor γ then scales with \bar{g} and is given by [50]

$$\gamma = \frac{4}{\pi \sin \theta} \frac{\bar{g}}{v_F^2}, \quad (28)$$

where θ is the angle between the directions of Fermi velocities at \mathbf{k}_{hs} and $\mathbf{k}_{hs} + \mathbf{Q}$.

The one-loop self-energy is the convolution of the bare fermionic Green's function $G_0(\mathbf{k}_{hs} + \mathbf{q}, \omega_m + \Omega_m)$ and

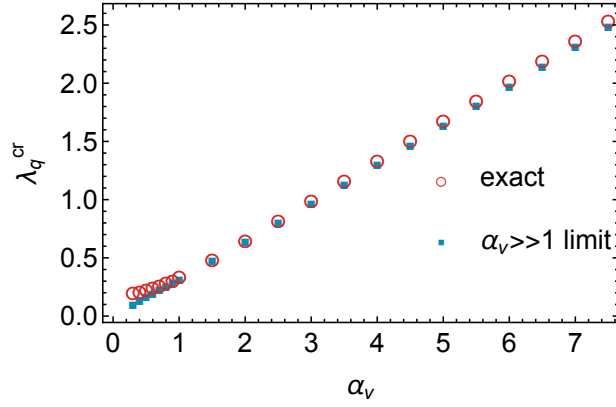


FIG. 9. Critical λ_q at different $\alpha_v = v_F/v_s$ for $\theta = \pi/2$. The spectral function shows pseudogap behavior for $\lambda_q < \lambda_q^{cr}$. Red circles are λ_q^{cr} , extracted from the exact formula for the one-loop self-energy, Eq. (29), and blue dots are obtained by using the approximate formula, Eq. (31), i.e., by solving Eq. (32).

$\chi(\mathbf{q}, \Omega_m)$. Expanding the dispersion to linear order in $\mathbf{q} - \mathbf{Q}$ and performing angular integration, we obtain

$$\Sigma(\mathbf{k}, i\omega_m) \approx -iv_F\xi^{-1} \frac{\lambda_q}{2\pi} \int dW_m \text{sgn}(w_m + W_m) \int \frac{dz}{\sqrt{z + (w_m + W_m)^2(z + 1 + \alpha_v^2 W_m^2 + \bar{\gamma}|W_m|)}} \quad (29)$$

where

$$\lambda_q = \frac{3}{4\pi} \frac{\bar{g}}{v_F \xi^{-1}} \quad (30)$$

and we introduced $w_m = \omega_m/(v_F\xi^{-1})$, $W_m = \Omega_m/(v_F\xi^{-2})$, $\bar{\gamma} = \gamma v_F \xi = \frac{16}{3 \sin \theta} \lambda_q$, and $\alpha_v = v_F/v_s$. At small λ_q , Landau damping is weak. Neglecting it, evaluating the frequency integral, and converting from Matsubara to real axis, we find that $\text{Im} \Sigma(\mathbf{k}, w)$ vanishes at $|w| < 1/\alpha_v$. At larger $|w|$, $\text{Im} \Sigma(\mathbf{k}, w)$ is non-zero. Substituting $\Sigma(\mathbf{k}, w)$ into the expression for the spectral function $A^q(\mathbf{k}_{hs}, \omega)$, we find that it has a maximum at $|w| \geq 1/\alpha_v$, i.e., at $|\omega| \geq v_s \xi^{-1}$. In the opposite limit of large λ_q , the Landau damping term is the strongest one in the spin propagator, and performing the same calculation we find that $A^q(\mathbf{k}_{hs}, \omega)$ has a broad peak centered at $\omega = 0$.

At large α , typical z in (29) are parametrically larger than $(w_m + W_m)^2$ (typical W_m is of order w_m). Neglecting $(w_m + W_m)^2$ and integrating over z , we obtain

$$\Sigma(\mathbf{k}, i\omega_m) \approx -iv_F\xi^{-1} \lambda_q \int_0^{w_m} \frac{dW_m}{\sqrt{1 + \alpha_v^2 W_m^2 + \bar{\gamma}|W_m|}} \quad (31)$$

Evaluating the remaining frequency integral, converting the self-energy onto the real axis, and evaluating the spectral function, we find analytically that pseudogap exists as long as $\lambda_q < \lambda_q^{cr}$, where the latter is the solution of

$$\lambda_q^{cr} = \frac{3 \sin \theta}{16} \frac{2}{\sqrt{3}} \sqrt{\frac{9 - 4\lambda^*}{5 - 4\lambda^* + (\lambda^*)^2}} \alpha_v. \quad (32)$$

where $\lambda^* = \lambda_q^{cr}/(1 + \lambda_q^{cr})$. Solving this equation, we find, at large α_v , $\lambda_q^{cr} = c\alpha_v$, where $c \approx (3 \sin \theta/16)\sqrt{10/3}$. We presented this result in the main text.

In Fig. 9 we compare λ_q^{cr} , obtained by using the full expression for the self-energy, Eq. (29), and by using the approximate Eq. (31), which we justified at large α_v . The same expression as (31) is obtained by factorizing the momentum integration along and transverse to the Fermi surface. This factorization is in turn justified if bosons are slow modes compared to fermions. We see from Fig. 9 that the values of λ_q^{cr} , obtained using the exact and the approximate forms of the self-energy, are essentially identical for all $\alpha_v \geq 1$.